BNL-222289-2021-TECH
NSLSII-ASD-TN-368

Feasibility Study of NSLS-II Sextupole BBA Measurement

J. Choi

October 2021

Photon Sciences
Brookhaven National Laboratory

U.S. Department of Energy
USDOE Office of Science (SC), Basic Energy Sciences (BES) (SC-22)

DISCLAIMER

NSLS II TECHNICAL NOTE BROOKHAVEN NATIONAL LABORATORY	NUMBER NSLSII−ASD−TN−368
AUTHOR **Jinhyuk Choi**	DATE 10/5/2021

Feasiblility Study of NSLS−II Sextupole BBA Measurement

Feasiblility Study of NSLS-II Storage Ring Sextupole BBA Measurement

Jinhyuk Choi

1 Introduction

In storage ring light sources, beam-based alignment (BBA) which adjusts the BPM centers to the quadrupole magnet centers is a common practice to maintain the machine performance. For more reliable and conveneint BBA process, in the design of the storage ring, BPMs are located as close as possible to the quadrupoles. The most common method is scanning the position of the beam at the BPM (equivalently at the adjacent quadrupole) and find the position where the quadrupole strngth change does not give change in the closed orbit.

While beam offsets in the quadrupoles give rise to the closed orbit distortions, offsets in sextupoles affect the overall machine performace, closed orbit, linear optics, couplicng and dispersion. Therefore, even though usually sextupoles are considered as the non-linear perturbation which corrects the chromatic effect and the effect can not-significant, we need to identify them and correct them if needed. Here, we would like to mention that the sextupole offset effects have different effects depending on the plane in which the beam is deviated and it makes the measurement more difficult.

Because the sextupole offsets changes various parameters, several different mathods can be used in measuring them. First, as in LOCO [3] the response matrix fit method is used [4] and proved to produce reliable results. In NSLS-II also, they have been measured [6] using ACLO [7] which adopts response matrix fit technique. For the LOCO or LOCO llike techniques to be successful, the machine is required to have a very trustful model and especially to measure the small sextupole effects the requirement is more strict. Furthermore, the measurement should have even higher signal-to-noise accuracy and results need to be confirmed in various ways. As other parameters, tune [1] and orbit changes [2, 5] can be used.

Compared to the quadrupole BBA, for the sextupole BBA, numerous complications are involved. First of all, there is no design consideration in locating BPMs and we cannot choose a BPM which can represent the beam position at the sextupole and accordingly there is no pairing between sextupoles and BPMs. Sencondly, the sextupole offset effects are not not stright-forward by including non-linear, as well as coupling, are also their strengths can be too weak to measure. And, finally, most serious complication involved for NSLS-II storage ring is that sextupoles are powered not individually but in family and that means when we want to measure the offset of a specific sextupole and change the current, all offsets in the same family affect the measurement.

In th simulation of the feasibility test, we choose parameters, tune, orbit and phase advance and measure their variations depending on the sextupole offsets. Also, together with the real configuration of family, we simulates the individual power supply case for the comparisons. In this note, the simulation processes and the results are presented.

2 Lattice Configuration

NSLS-II storage ring consists of 15 super-cells where each super-cell has two cells with the mirror symmetry and 3 super-cells are forming 1 pentant. The lattice configuration one super-cell of the NSLS-II storage ring is shown in Fig. 1.

As a double-bend achromat lattice, each cell has 2 dipoles and there are 10 quadrupoles, 9 sextupoles, 6 correctors, and 6 BPMs. In addition to the multipoles, 3 damping wigglers are installed at ID sections of cell 8, 18 and 28 to reduce the emittance. As the main lattice element, each quadrupole has its own

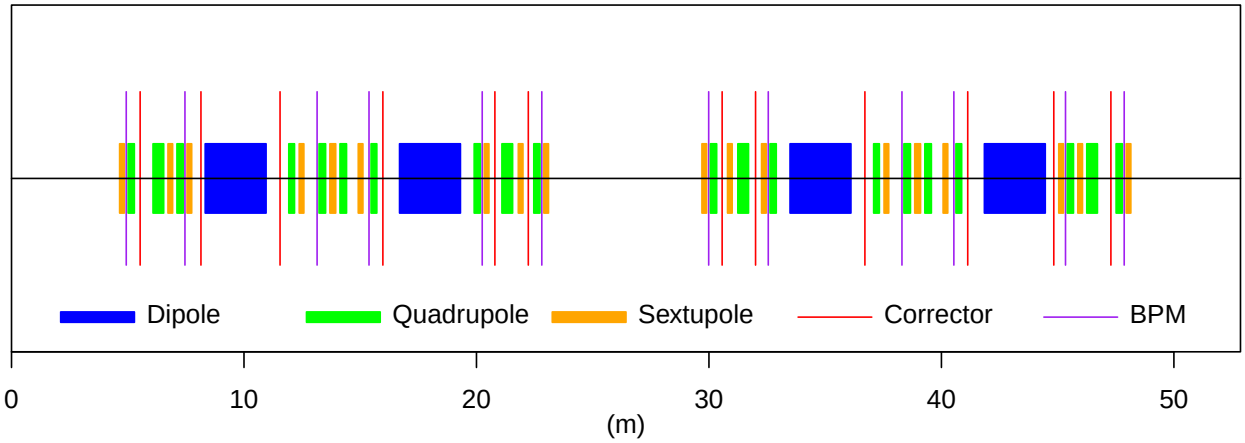

Figure 1: Lattice configuration of 1 super-cell of NSLS-II storage ring.

power supply but the sextupoles are serially connected and make families with one power supply for one family. Even though all super-cells are equivalent in model, for the flexibility, NSLS-II storage ring has independent 9 families for each pentant, resulting 45 sextupole families. Additionally, because the symmetry is broken by the damping wigglers, sextupoles surrounding the damping wigglers have their own power supplies and the number of families increase by 9. As the result, the total number of of sextupole families is 54 and no 2 sextupoles in one cell belong to one family.

When we measure the quadrupole BBA, because each magent has its own power suppy, we just focus on the beam position at the quadrupole not caring about the position at other quadrupoles. But for sextupoles, because they are powered in family, we need to make local bump around the specific sextupole so that the variations of other same familiy sextupoles' strengths do not affect the measured data. Theoretically, the methods making 3-bump or 4-bump are very simple and well established. From the lattice configuration shown in the Fig. 1 where every adjacent corrector pair is surrounding 0, 2 or 3 sextupoles, it is not possible to make the isolated local bump including single sextupole. Similarly, each adjacent pair of BPMs is surrounding 0 or 2 sextupoles. However, except the ones at the ends of the cells, we can make 4-bump including only one member of the sextupole family. For those at the ends of cells, if they belong to the same pentant, no bump can includes a single family member unless the pentants are changing at those cells. In that case, they belong to different families and the can be powered separately.

In fact, 4-bumps can be effectively generated by global orbit response matrices by assigning non-zero target values only for the surrounding BPMs. This is convenient as well as robust because the measured response matrices are always available. Therefore, we will use 4-bumps for the offset scan at the sextupoles and, that means, for those at the ends, we can only measure the average offsets.

3 Simulation

In the note, as the first step to prepae the measurements, the machine is considered as having no other error except the sextupole offsets. The sextupoles are, different from the offsets in main quadrupoles, intstalled to correct the chromatic effects and themselves are considered as the non-linear perturbations from the point of beam dynamics. Therefore, it can be easily expected that measuring their offsets cannot be as straight-forward as in the case of measuing the quadrpole offsets. The sextupole offsets can make various perturbation in linear and non-linear optics and we review some of the effects on the lattice by simulation.

First, based on the design specification and the survey daya, we used normal distributed random numbers having 100 μm as the standard deviation for the sextupole offsets. They are assigned to both planes independently without any cut-off values. These offsets introduce the closed orbit distortions as well as changes in phases. and, even though the orbit distortion is quite small, we correct them first and then we add the local bumps to scan the beam orbit at sextupoles. The design x/y tunes of the NSLS-II

storage ring are 0.221/0.26. To simulate as close as to the real machine, we applied family configuration of the sextupole and quadrupole with individual unit-conversion tables. This process give sllight changes in the design tune but not shown in the significant digits. On top of this adjustment, the random offsets are given and the shifted tunes x/y from the sextupole offsets become 0.211/0.264.

Tunes are simple and direct measures of the sextupole offsets, but the fact that having only 2 points give reliability issue in the real measurements. As the feasibility study, we also review the effects on the orbit and changes in phase advances between all the BPMs. We would like to note that the phase advances can be measured quite accurately using the turn-by-turn data. As the sextupoles are powered by families, when a given algorithm cannot predict the real deviations, it is not easy to tell it is from the family issue or unsatisfacotry algorithm. To make it clear, we repeat every simulation with and without family configuration. To see the effects of all kinds of families, we perform the offset measuremt simulation for the sextupoles in cell 7 and 8 where the 3 pairs of sextupoles surrouning the DW08 make their own families. In the following subsections, we describe the bump generations and display the simulation results when we use the the tunes, orbits, and the phase advances as the changing parameters from the sextupole offsets.

3.1 Local bumps

The name of sextupole in cell 7 through 8 are as follows.

SL1G2C07A, SL2G2C07A, SL3G2C07A, SM1G4C07A, SM2G4C07B, SM1G4C07B
SH4G6C07B, SH3G6C07B, SH1G6C07B, SH1G2C08A, SH3G2C08A, SH4G2C08A
SM1G4C08A, SM2G4C08B, SM1G4C08B, SL3G6C08B, SL2G6C08B, SL1G6C08B

Among them the pairs (SH4G6C07B, SH4G2C08A), (SH3G6C07B, SH3G2C08A), (SH1G6C07B, SH1G2C08A) have their own power supplies and all other magnets belong to the pentant families. In making the local bumps for these magnets, the families are not considered. Taking account of the fact that assigned offsets' standard deviation is $100\mu m$, we limit the local bumps to $\pm 300\mu m$. Using the response matrices, we can obtain the horizontal and vertical local bumps of this range without any issue for all the sextupoles under study. The bumps are scanned at 4 steps as $(-300\mu m, -100\mu m, +100\mu m, +300\mu m)$, and the implemented horizontal and vertical bumps at SM2G4C07B and SM2G4C08B together with the corresponding corrector currents are shown in Fig. 2. Also, it needs to be noted that if the measured value of the simulation goes beyond the scan range, the corresponding scan limit is logged as the result. At each step of the bump scan, variable changes are measured when the corresponding sextupole currents are increased by 20 A.

3.2 Tune variations

The local bumps which give the minimum tune shifts are estimated both for the individual power supply and family connection cases. Because of the coupling, the offset in one plane can be also estimated using the tune variation of the other plane. The horizontal tune variations depending on the bump height for the individual power supply case are shown Fig. 3. In the figure, the two lines of the same color represent the horizontal and vertical tune variations for the given sextupole. The crossing points of $\delta\nu$ give the measured offsets and collected in Fig. 4.

The horizontal offsets when assuming the individual power supplies, the data are quite clear and the obtained estimations are also very accurate. However, the vertical offset data are, even under the individual assumption, quite noisy and the result is useless as shown in Fig. 5.

The results when we apply the power supply family connections, are shown in Figs. 6 through 8. Even though they are not so satisfactory, they are not absolutely meaningless in the horizontal plane but, in the vertical plane, the measurements seem to have no point.

3.3 Orbit variations

The sextupole offsets are estimated using the effects on the orbit from the offsets. The number of lines becomes too many to show all of them and the horizontal offset data when the individual power supply is assumed for the sextupole SM2G4C07B are shown in Fig. 9. 10. The data from the horizontal orbit changes

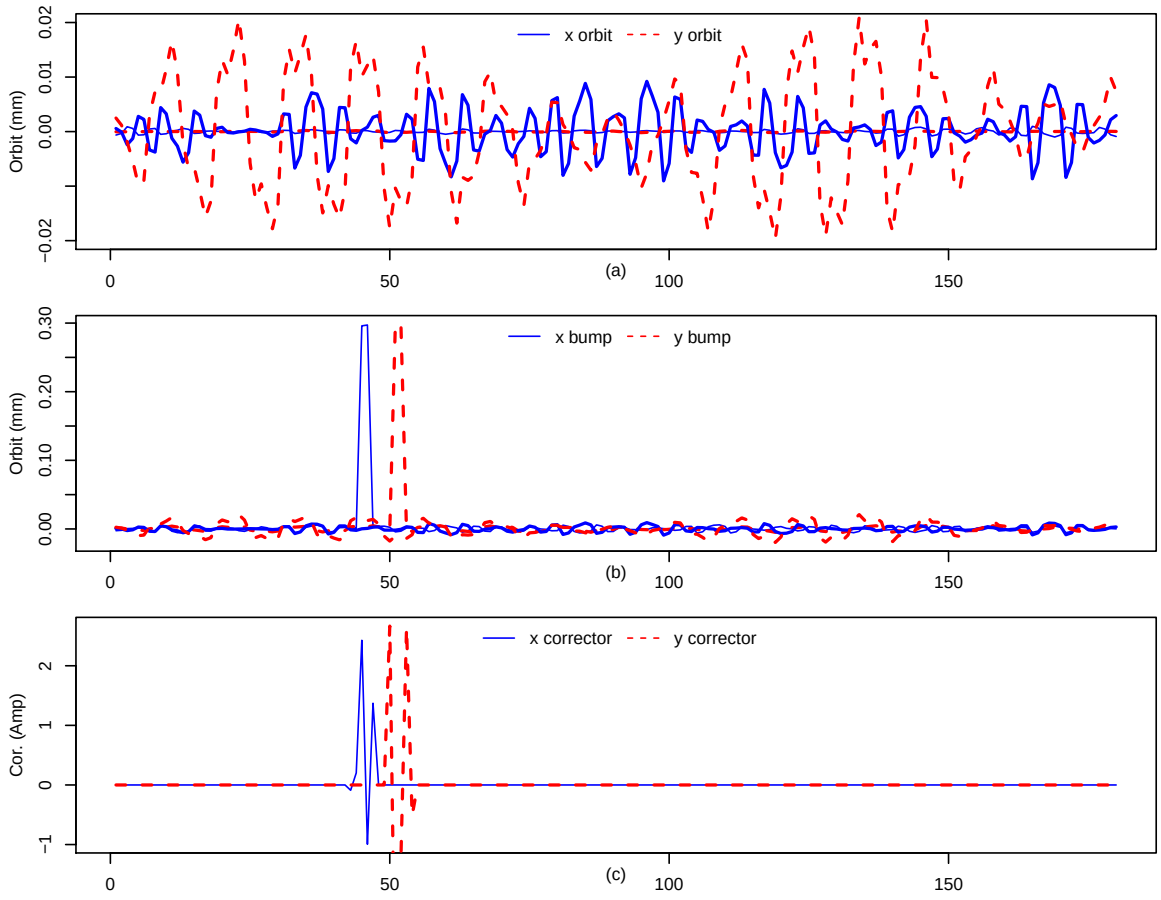

Figure 2: (a) Disturbed orbits due to the sextupole offsets and the corrected ones. (b) Horizontal and vertical local bumps on top of the corrections at SM2G4C07B and SM2G4C08B. (c) Required corrector strengths. They are well within the available ranges unless the set-point is already at the edge.

have some width but the solutions are quite satisfactory. Especially, measurements using the vertical orbit changes are very clear (Fig. 11, 12) but the changes are too small for the real measurements. Result for the vertical offsets are also satisfactory. With the power supply famiies applied, the data and the results are shwon in Fig. 14 through Fig. 16. Even with the large error bars, we can see the meaningful resuls in both planes.

3.4 Changes in Phase Advances

As the final method, we use the changes of BPM to BPM phase advances depending on the sextupole offsets. The data and the offset estimations without and with power supply families are shown in Fig. 17-24. We can see that not all the phase advances are affected by the bump scans and we can see the size of error bars are different sextupole to sextupole. It is noted that even in the case, especially in the vertical phases, when the data look non-systematic, the estimated result could be meaningful. The advantage by taking the phase advances as the measurement parameters is that, as mentioned, the phase advances can be measured in very high accuracy from the turn-by-turn data..

4 Summary

Three methods are simulated to measure the sextupole offsets, using tune, orbit and phase changes as parameters. Tune changes work more or less in measureing the horizontal offsets but, for the vertical offsets, no information can be obtained. Furthermore, to collect the statistically meaningful data, the measurement need be repeated many times and the hysteresis effect can affect the data reliability. In fact, all the parameter changes can be obtained together, we will see the effects anyway.

The orbit and phase advances seem to provide relatively good tools to measure the offsets. However, we expect difficulties about their reliability due to the large error bars and tiny changes, especially in the vertical orbit changes. Adjusting the sextupole strength step, as other than 20 A affect the result little and if it becomes too high, the non-linear effects dominate and if it is too low, the effects becomes too week. The optimum value can be searched in the real measurements.

With the simulation without any other erros, we estimated the expected results for various methods and found proper parameter values to use at the starting phase of the real measurements. At the same time, we will perform the simulations with the realistic errors and use the results to improve the productivity of the real measurements.

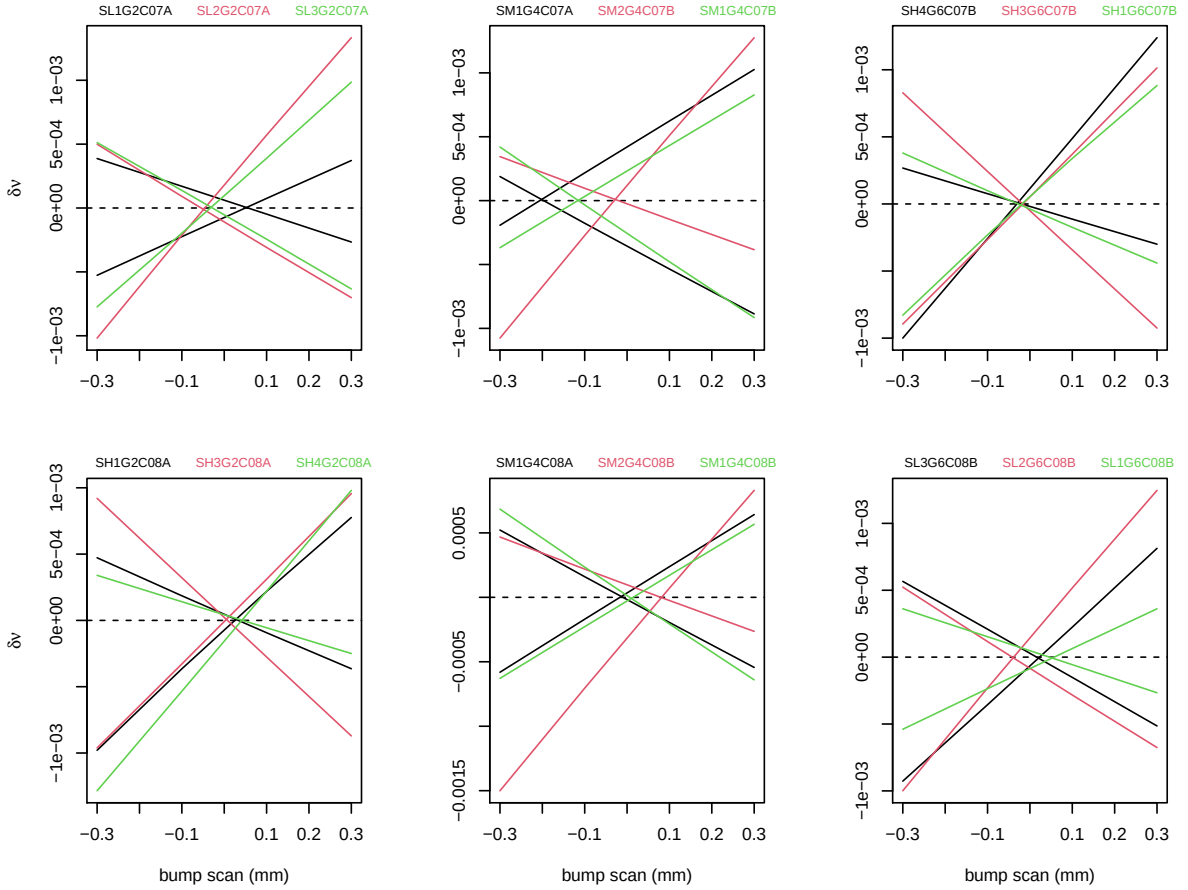

Figure 3: Horizontal tune variations when individual power supplies are assumed. The same colors represent horizontal and verical tune shift from the sextupole strenght change for the given sextupole while bump heights are scanned.

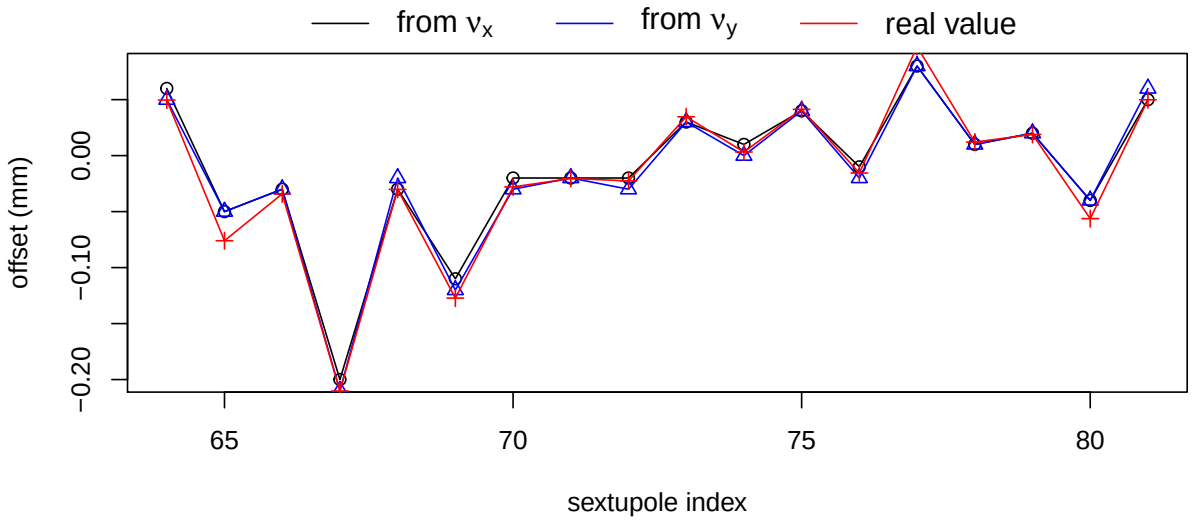

Figure 4: Results for the horizontal offset measurements using the tune variations when individual power supplies are assumed.

References

[1] M. Borland. Measurement of sextupole orbit offsets in the aps storage ring. In *Proceedings of the 1999 Particle Accelerator Conference*, pages 1587–1589, 1999.

[2] Yu-Chiu Chao. A Technique for Aligning Sextupole Systems. 1992.

[3] J. Safranek. Experimental determination of storage ring optics using orbit response measurements. *Nucl. Instrum. Meth. A*, 388:27–36, 1997.

[4] V. Sajaev and A. Xiao. Simultaneous measurement of all sextupole offsets using the response matrix fit. In *Proceedings of the 2010 International Particle Accelerator Conference*, pages 4737–4739, 2010.

[5] A. Xiao and V. Sajaev. Beam-based alignment of sextupoles at the aps. In *Proceedings of the 2013 Particle Accelerator Conference*, pages 463–465, 2013.

[6] X. Yang. Applying multi-frequency ac loco for finding sextupole erros. *NSLS-II Technical Note*, (NSLSII-ASD-TN-342), 2020.

[7] X. Yang, Smaluk V., L.H. Yu, and K. Ha. Multi-frequency ac locl: A fast and precise technique for lattice correction. In *Proceedings of the 2010 International Particle Accelerator Conference*, pages 831–834, 2017.

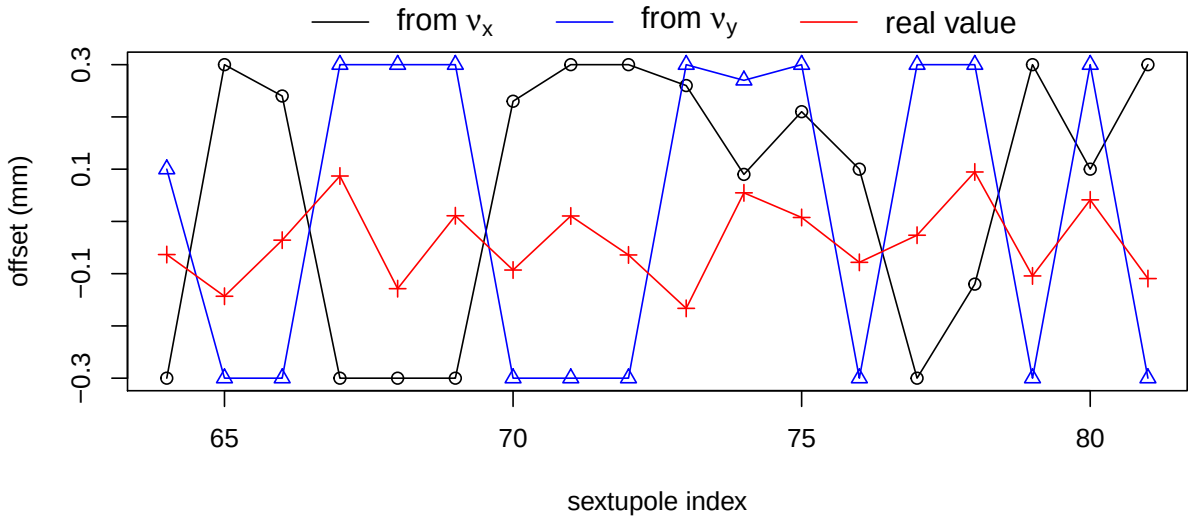

Figure 5: Results for the vertical offset measurements using the tune variations when individual power supplies are assumed.

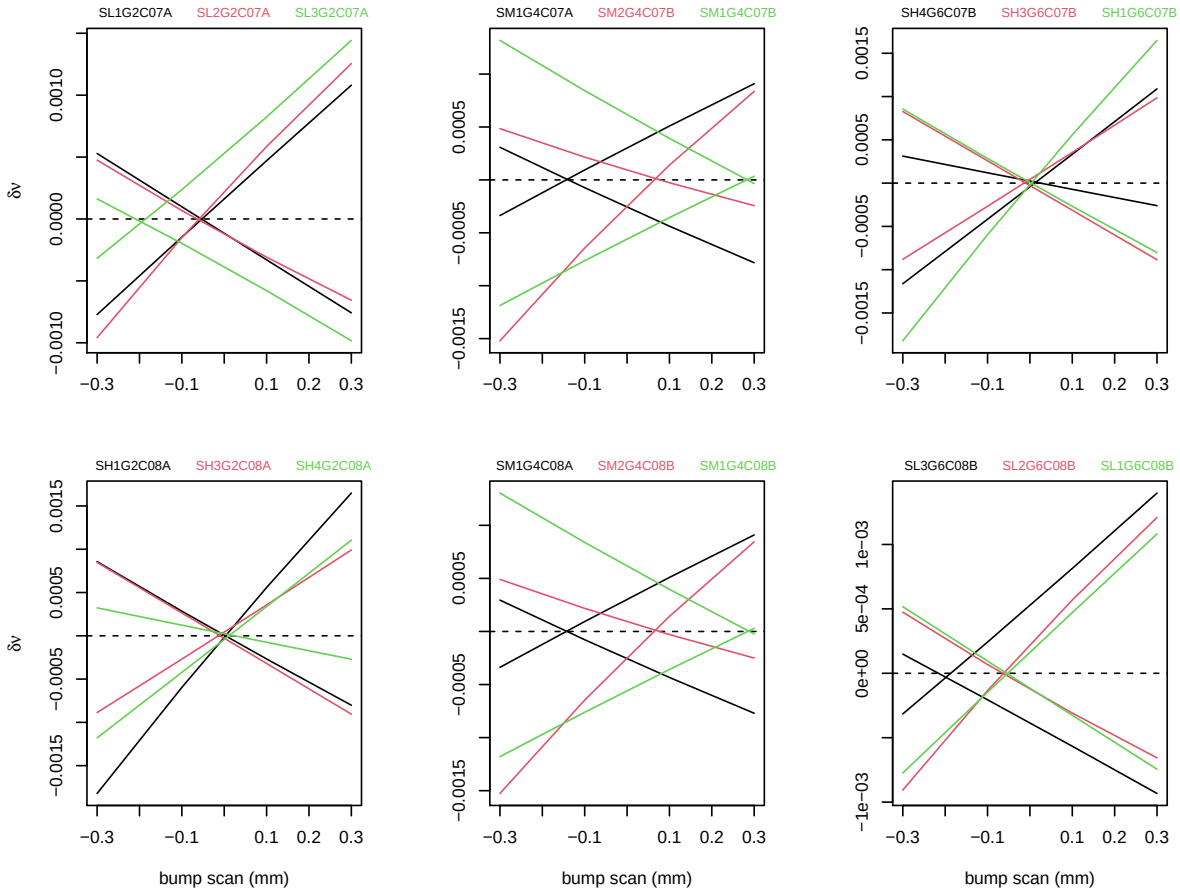

Figure 6: Horizontal tune variations when family connections to the power are applied. The same colors represent horizontal and vertical tune shift from the sextupole strenght change for the given sextupole while bump heights are scanned.

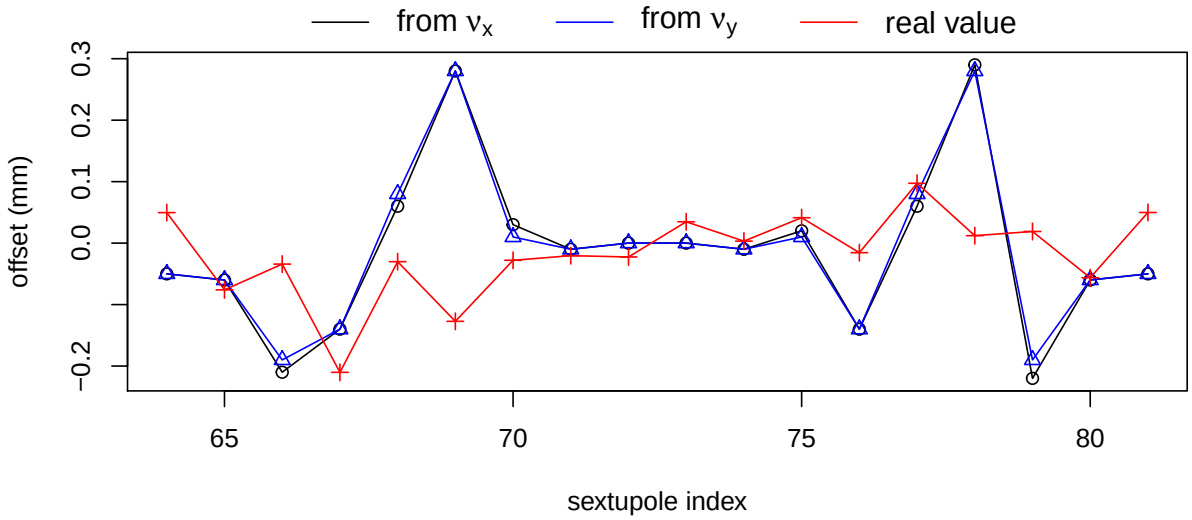

Figure 7: Results for the horizontal offset measurements using the tune variations when family power supplies are applied.

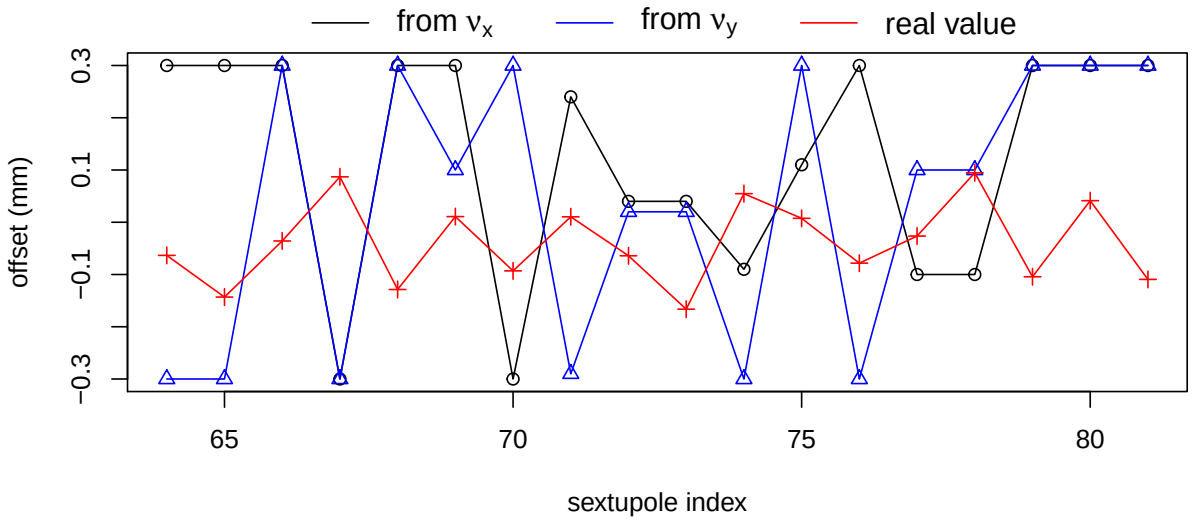

Figure 8: Results for the vertical offset measurements using the tune variations when family power supplies are applied.

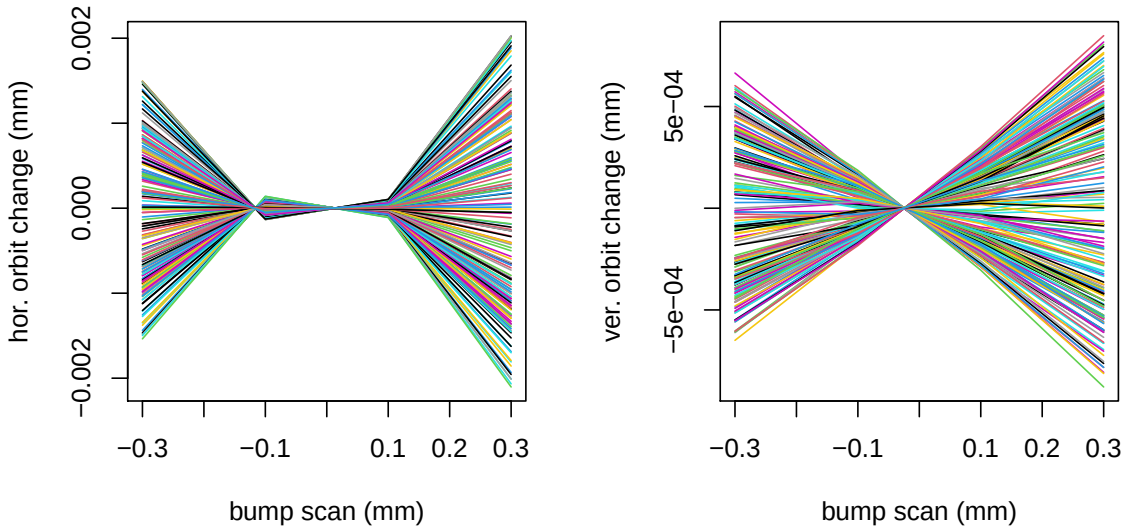

Figure 9: Horizontal and vertical orbit changes depending on horizontal offset at SM2G4C07B.

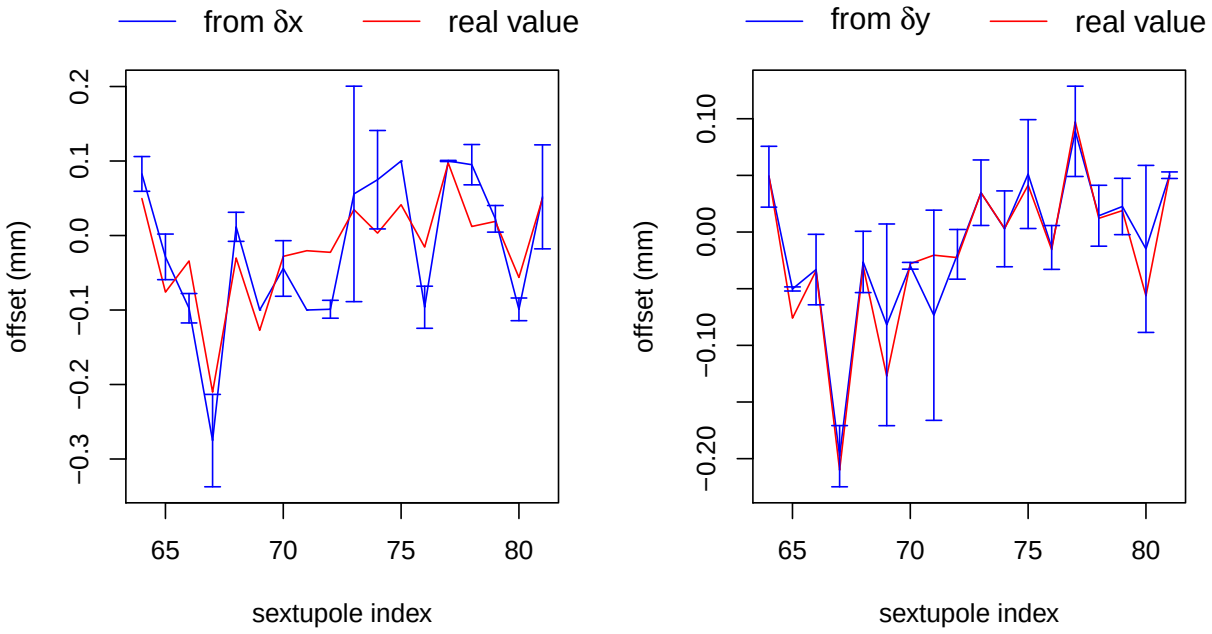

Figure 10: Estimated horizontal offsets using orbit changes (individual power supplies).

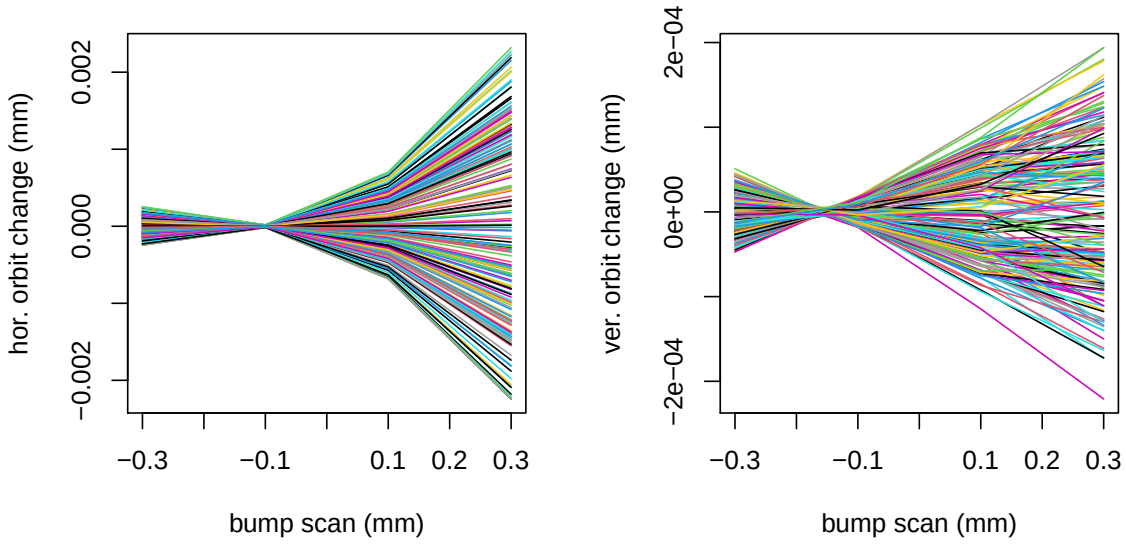

Figure 11: Horizontal and vertical orbit changes depending on vertical offset at SM2G4C07B.

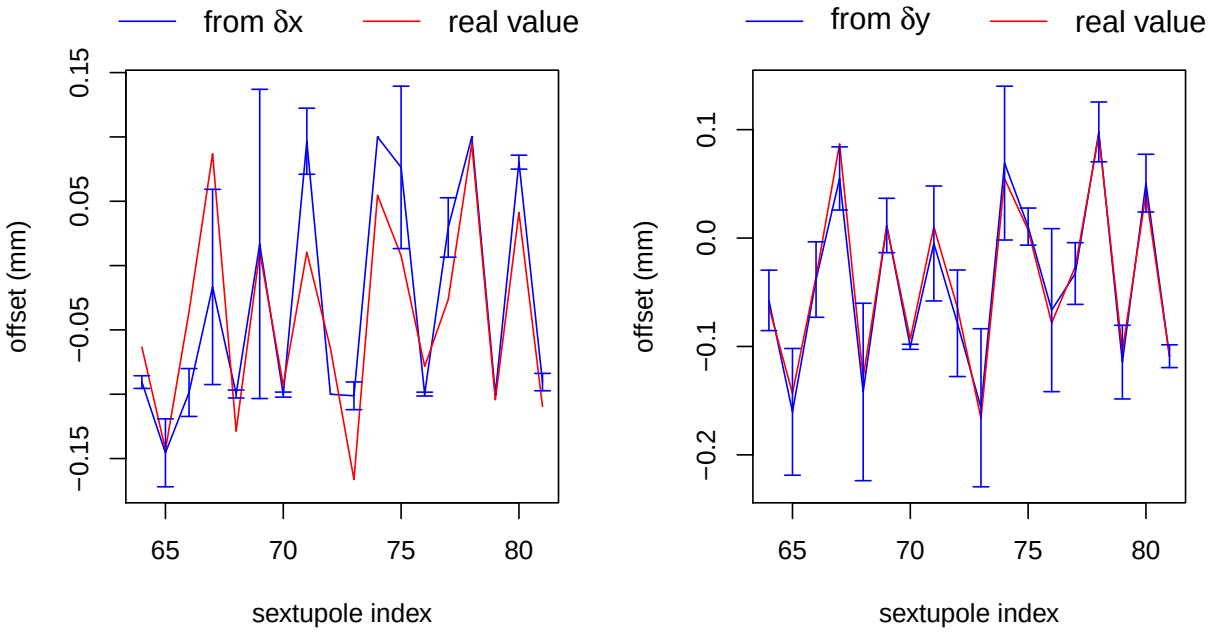

Figure 12: Estimated vertical offsets using orbit changes (individual power supplies).

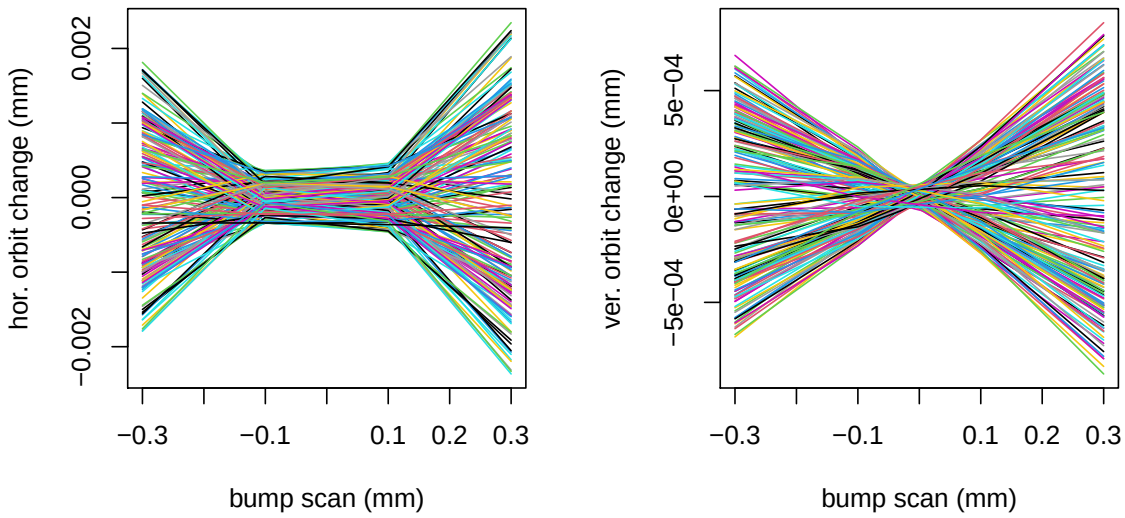

Figure 13: Horizontal and vertical orbit changes depending on horizontal offset at SM2G4C07B.

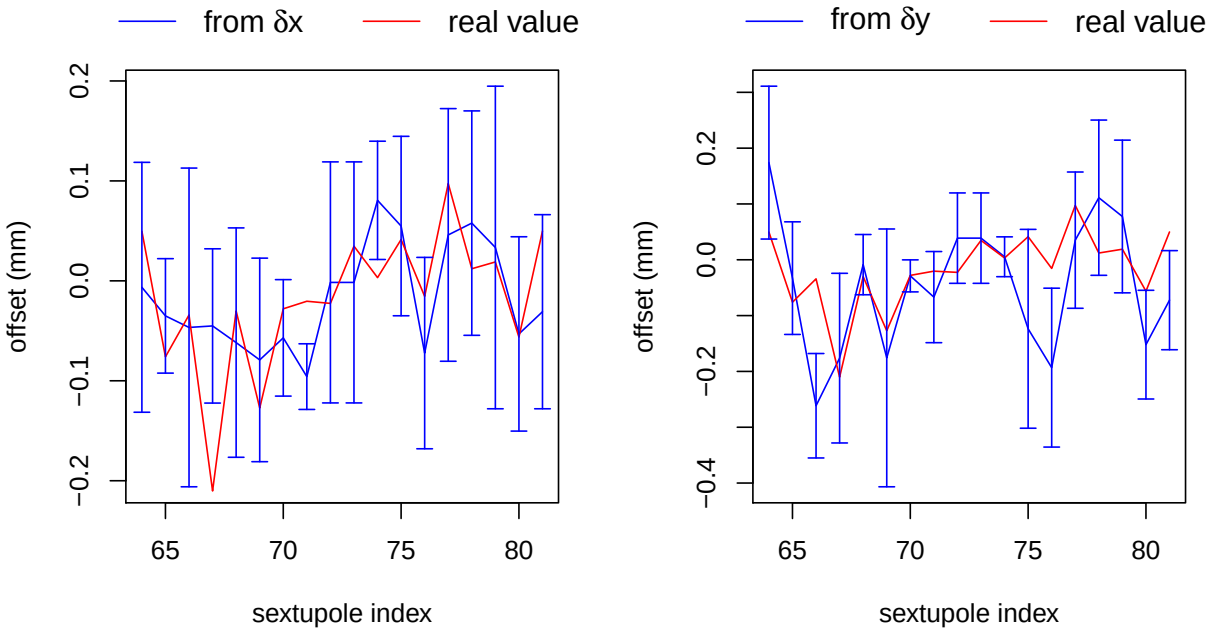

Figure 14: Estimated horizontal offsets using orbit changes (family applied).

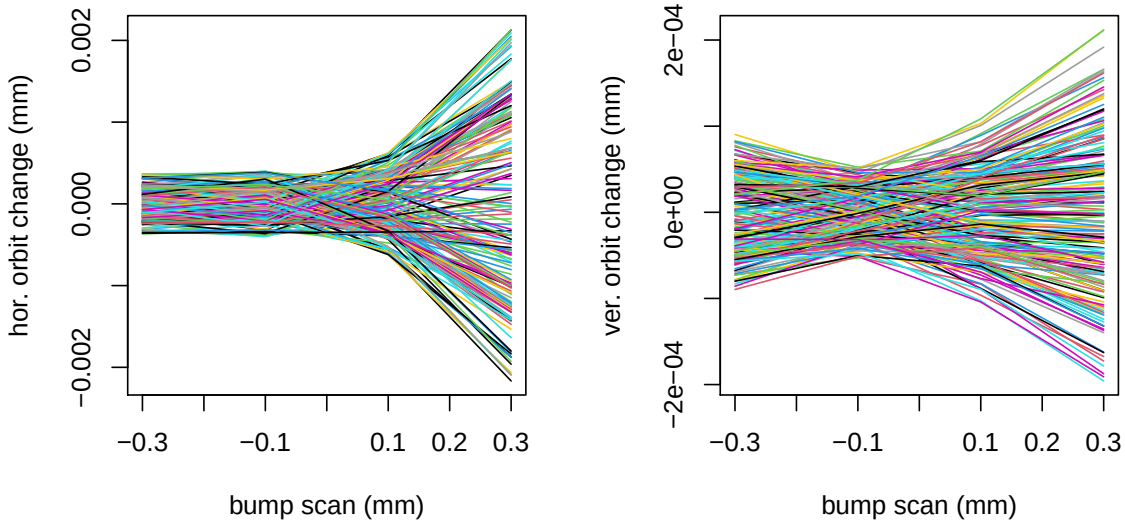

Figure 15: Horizontal and vertical orbit changes depending on vertical offset at SM2G4C07B.

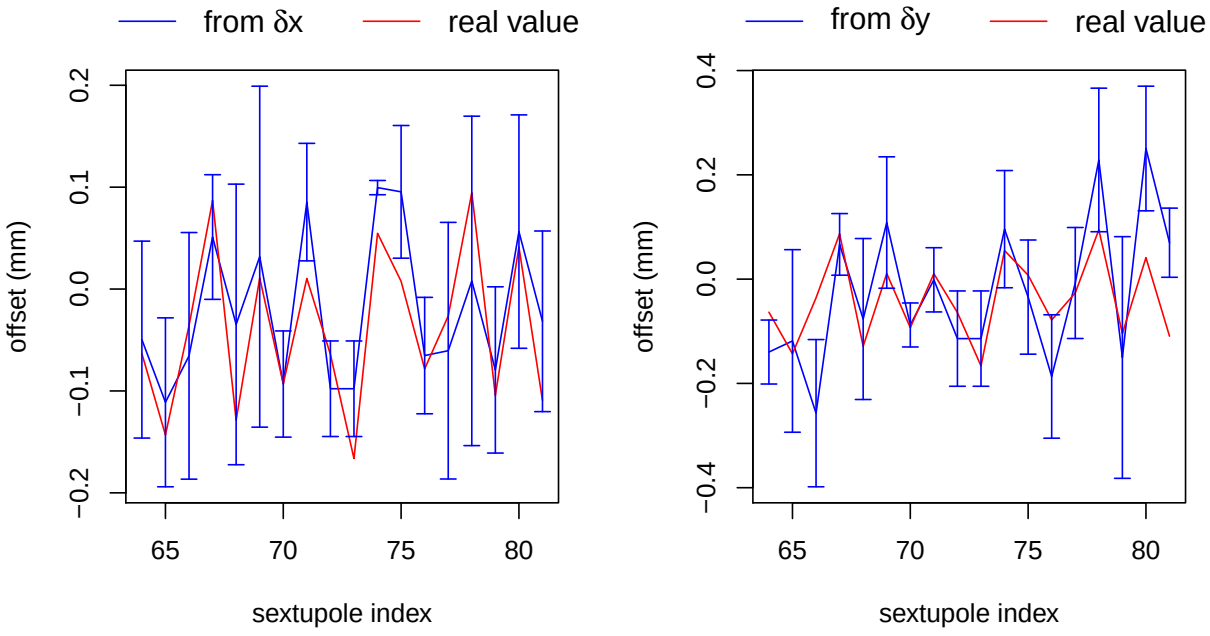

Figure 16: Estimated vertical offsets using the orbit changes (family applied).

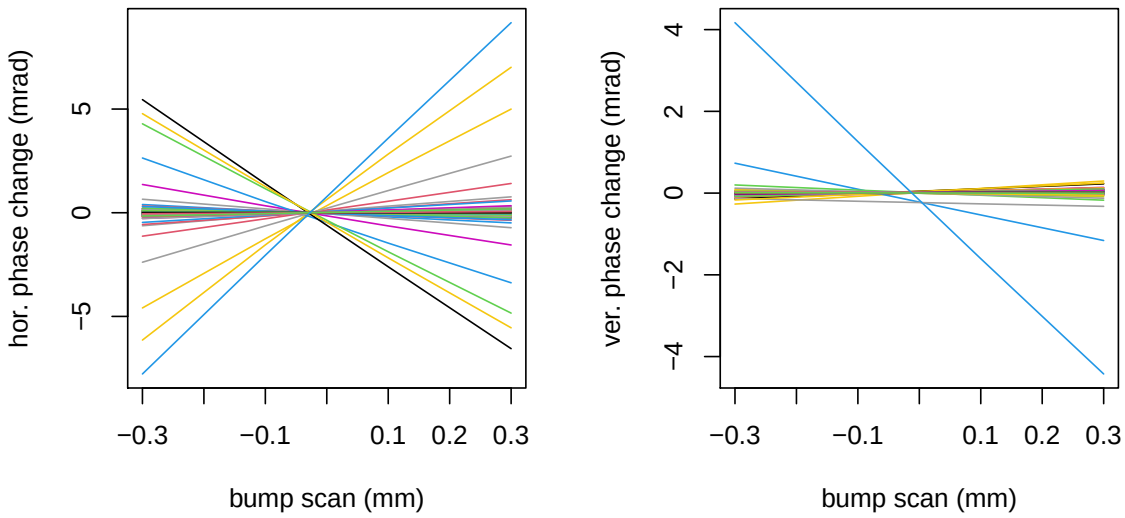

Figure 17: Horizontal and vertical phase changes depending on horizontal offset at SM2G4C07B.

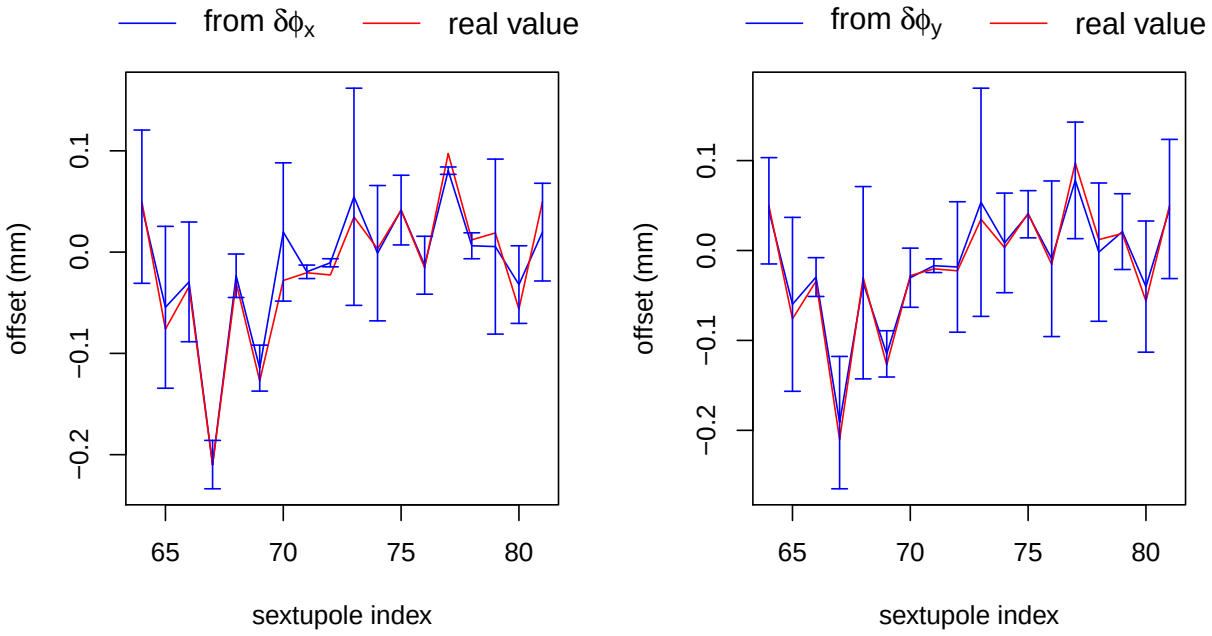

Figure 18: Estimated horizontal offsets using the phase changes (individual power supplies).

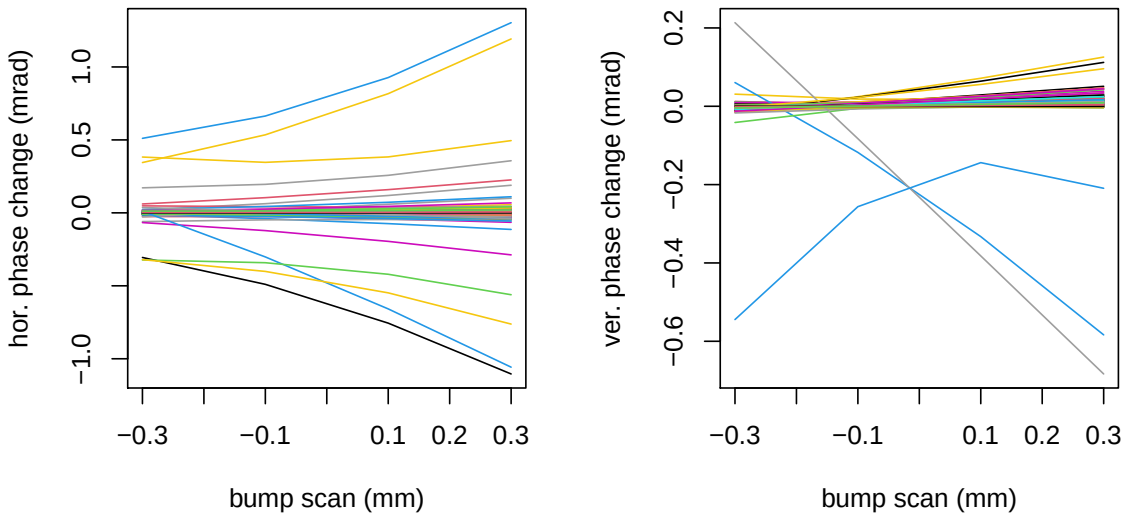

Figure 19: Horizontal and vertical phase changes depending on vertical offset at SM2G4C07B.

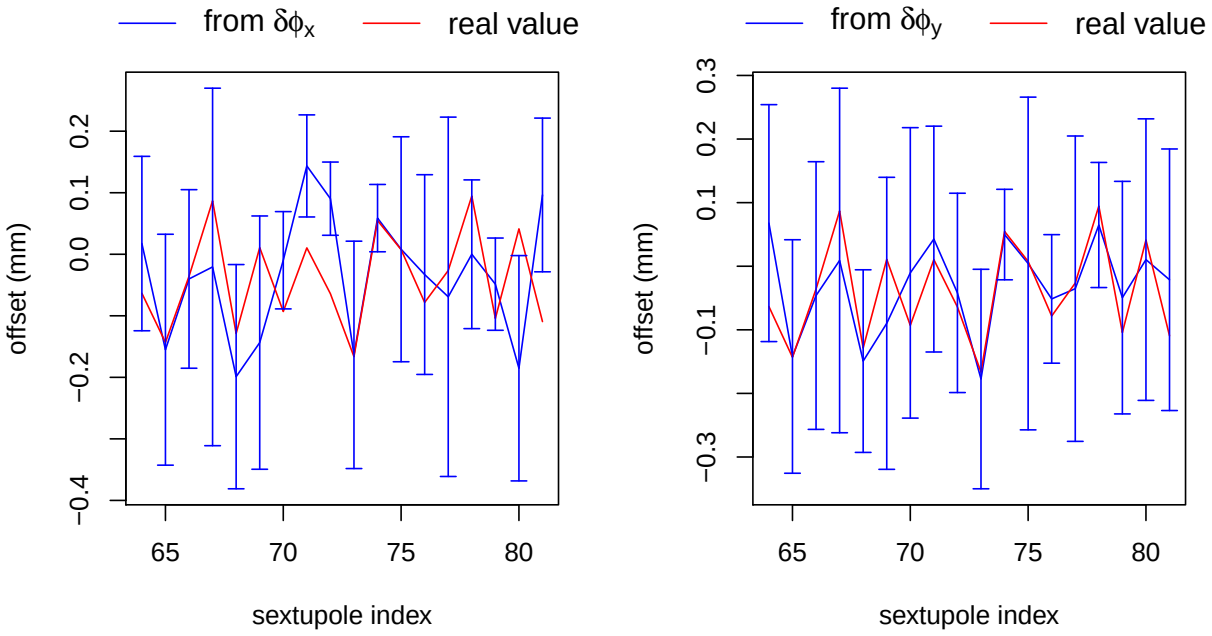

Figure 20: Estimated vertical offsets using the phase changes (individual power supplies).

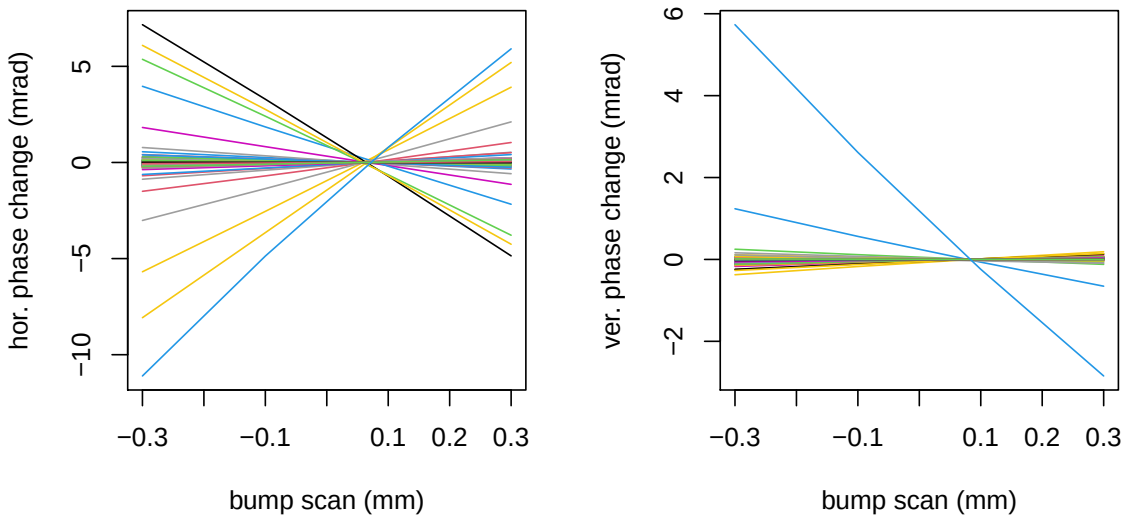

Figure 21: Horizontal and vertical phase changes depending on horizontal offset at SM2G4C07B.

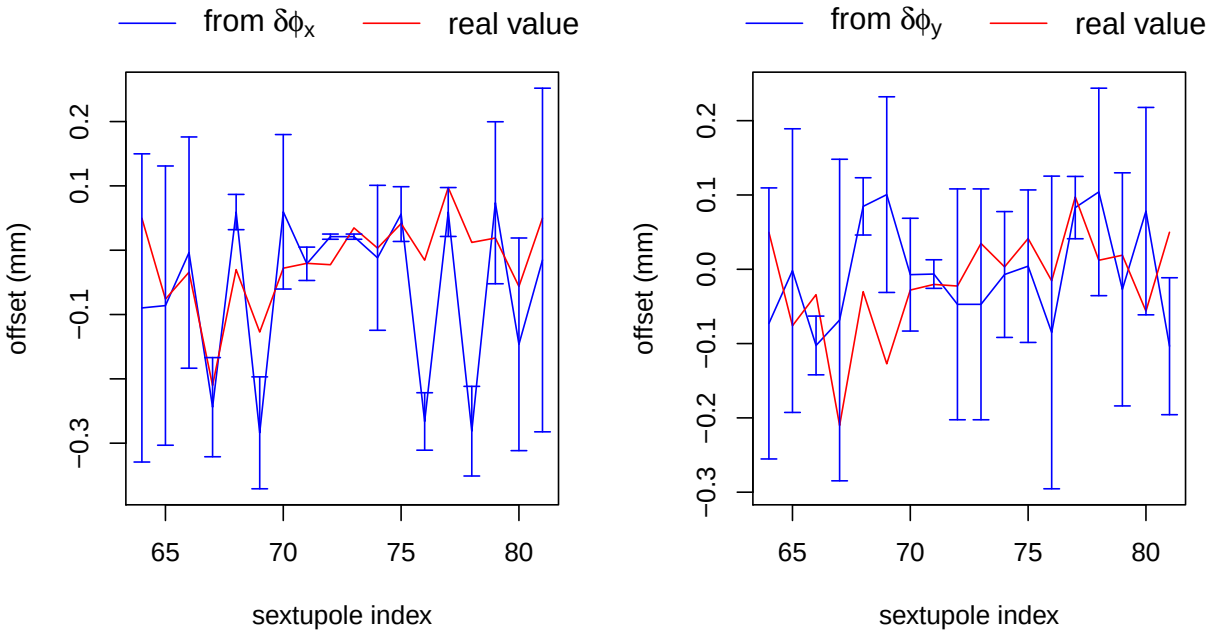

Figure 22: Estimated horizontal offsets using the phase changes (family applied).

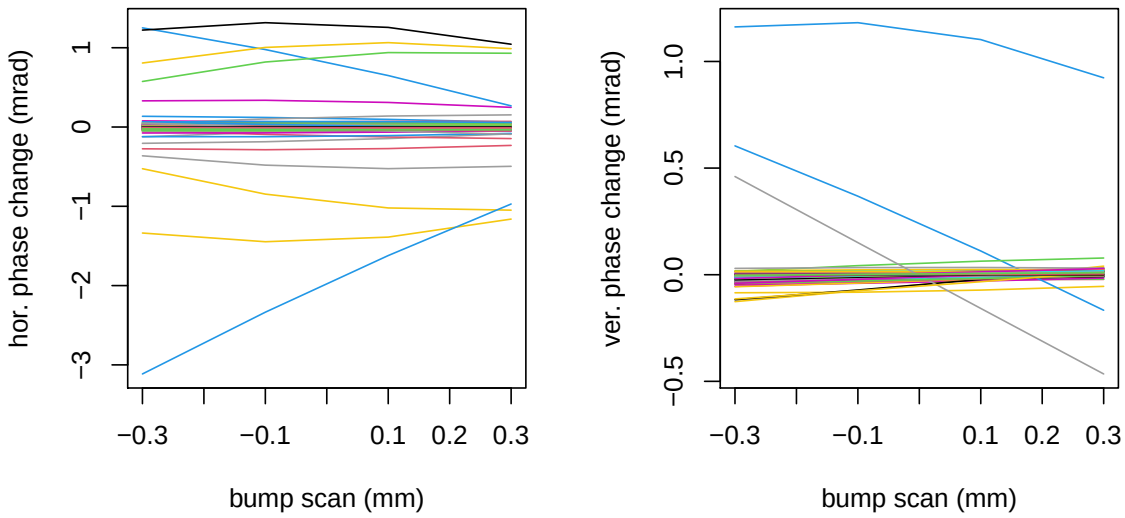

Figure 23: Horizontal and vertical phase changes depending on vertical offset at SM2G4C07B.

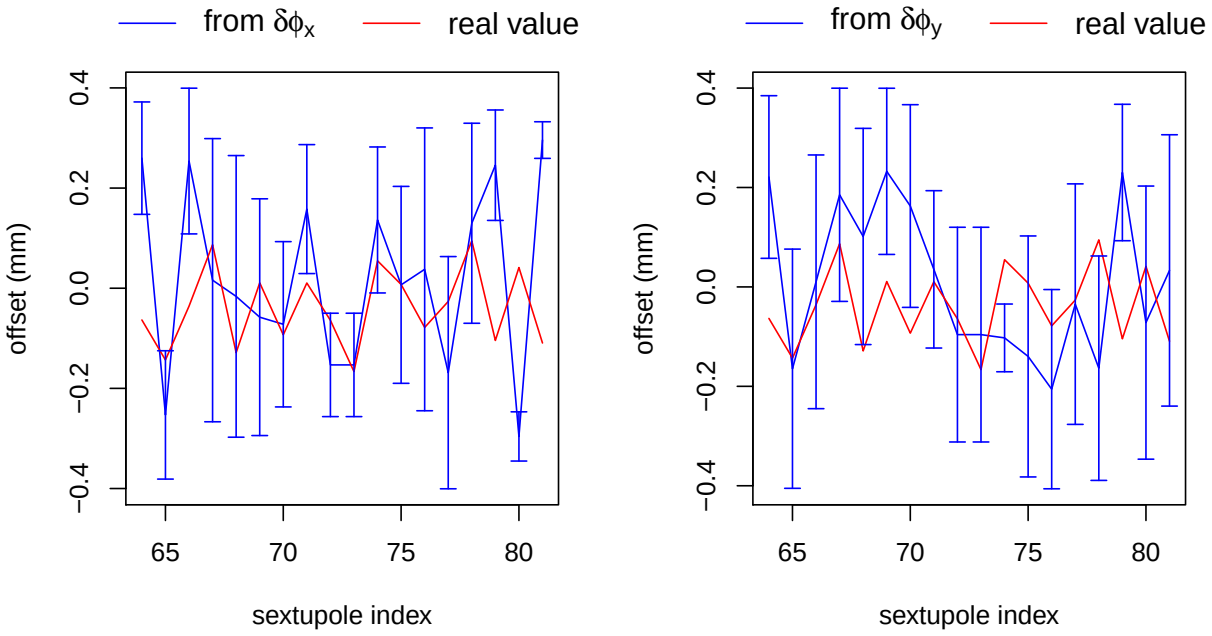

Figure 24: Estimated vertical offsets using the phase changes (family applied).